Journal of Glaciology

Air trajectories and snowfall over Alaska–Yukon icefields: implications for ice-core accumulation studies

Ingalise Kindstedt[1,2], Dominic Winski[1,2], Luke Copland[3], Michael G. Loso[4], Karl Kreutz[1,2] and Christian Zdanowicz[5]

[1]School of Earth and Climate Sciences, University of Maine, Bryand Global Sciences Center, Orono, ME, USA; [2]Climate Change Institute, University of Maine, Orono, ME, USA; [3]Department of Geography, Environment and Geomatics, University of Ottawa, Ottawa, Ontario, Canada; [4]Inventory and Monitoring Program, Wrangell-St. Elias National Park and Preserve, National Park Service, Copper Center, AK, USA and [5]Department of Earth Sciences, Uppsala University, Uppsala, Sweden

Article

Cite this article: Kindstedt I, Winski D, Copland L, Loso MG, Kreutz K and Zdanowicz C (2026) Air trajectories and snowfall over Alaska–Yukon icefields: implications for ice-core accumulation studies. *Journal of Glaciology* **72**, e41, 1–11. https://doi.org/10.1017/jog.2026.10142

Received: 21 August 2025
Revised: 15 December 2025
Accepted: 26 February 2026

Keywords:
accumulation; glacier meteorology; ice and climate; ice core; snow

Corresponding author: Ingalise Kindstedt; Email: ingalise.kindstedt@maine.edu

Abstract

Glaciers surrounding the Gulf of Alaska contain records of past climate. However, interpreting records from the region's interior vs maritime mountain ranges is challenging, partly due to uncertainties in air transport associated with snowfall. Here, we combine in situ snow accumulation data and back trajectory modeling to examine air-parcel trajectories associated with snowfall in the St. Elias and Alaska Ranges, and their implications for climate records contained in glacier ice. We find that orographic effects lead to dissimilar accumulation patterns between the interior Alaska Range and maritime St. Elias, with the greatest influence during low-intensity snowfall. High-intensity storms tend to affect the entire region, while low-intensity snowfall requires a break in the coastal mountains to access inland sectors. Results suggest the regional precipitation regime will evolve with changes in storminess in and around the Gulf of Alaska. Specifically, we expect overall higher regional snowfall, but possible changes in distribution depending on future storm tracks. Finally, results indicate the divergence between St. Elias and Alaska Range ice-core accumulation records since ~1400 C.E. may be explained by a shift in dominant parcel trajectory, rather than an increase in storm strength or frequency.

1. Introduction

The Gulf of Alaska region, which includes Alaska, Yukon and parts of British Columbia, contains over 40 mm of sea level equivalent in its many alpine glaciers and icefields (Farinotti and others, 2019). The region also contains one of the planet's most dramatic barriers to inland transport of coastal moisture, with peaks exceeding 5000 m a.s.l. located less than 100 km from the coast (Newman and others, 2020). Orographic precipitation resulting from this topography feeds the icefields of coastal mountain ranges and the glaciers that drain them (Marcus and Ragle, 1970). High-alpine glaciers are also found in the region's interior, most notably in the Alaska Range (central Alaska, Fig. 1).

The proximity of coastal and interior glaciated alpine sectors in the Gulf of Alaska region has presented opportunities to collect a unique suite of ice-core climate records located close to one another, but spanning distinct climate regimes (Fisher and others, 2004; Yalcin and others, 2007; Bieniek and others, 2012; Zdanowicz and others, 2014; Tsushima and others, 2015; Osterberg and others, 2017; Winski and others, 2017; Fang and others, 2023). Such cores provide hundreds of years of climate data at sub-annual resolution, with additional deeper, lower-resolution ice reaching as much as 30 000 years in age (Fisher and others, 2004; Zdanowicz and others, 2014; Fang and others, 2023). However, the heterogeneity of the terrain challenges interpretation of such records; sites in relatively close proximity may be subject to different atmospheric processes, moisture sources and depositional mechanisms. This may result in dissimilar climate records that can, when used together, provide a more nuanced picture of regional climate than the record from any one site alone.

For example, a doubling of snow accumulation recorded in an ice core from the Begguya summit plateau (We use the indigenous name 'Begguya', rather than the more recent 'Mt. Hunter', Fig. 1c) between approximately 1840 and 2016 has been interpreted to reflect a combination of regional atmospheric warming and concurrent strengthening of the Aleutian Low (Winski and others, 2017), which could occur due to greater duration or strength of individual storms, higher storm frequency, greater coherence between individual storm trajectories to a well-defined track, or some combination. However, an unresolved question is why the Begguya

https://doi.org/10.1017/jog.2026.10142 Published online by Cambridge University Press

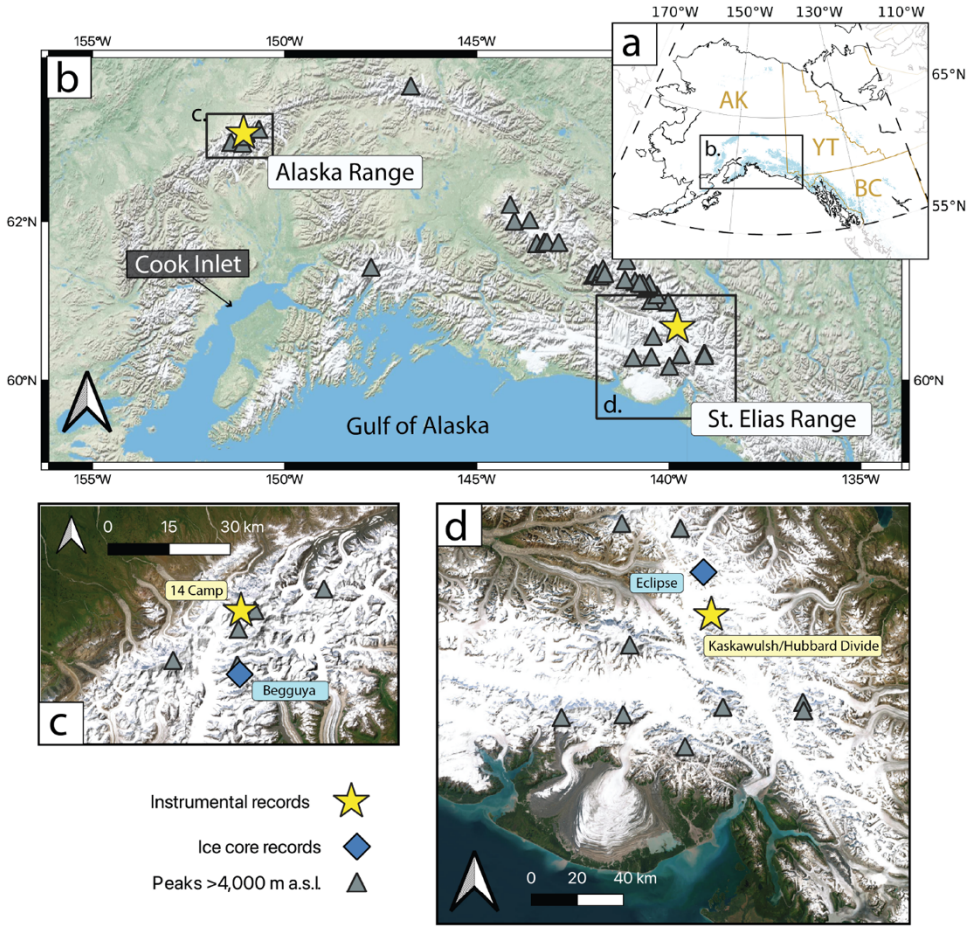

Figure 1. Study sites in the Gulf of Alaska region. Instrumental accumulation records are marked with yellow stars; ice-core locations discussed in this study are marked with blue diamonds. Peaks $> 4,000$ m a.s.l. are marked with gray triangles. The Alaska (AK), Yukon Territory (YT) and British Columbia (BC) borders are shown in gold in panel (a). Panel (c) shows study sites in the Alaska Range; panel (d) shows study sites in the St. Elias Range. Stars in the Alaska Range and St. Elias Range in panel (b) correspond to 14 Camp and Divide, respectively.

accumulation record shows such a distinct increase, while a concurrent regional ice-core record from Eclipse Icefield (Kelsey and others, 2012) does not (Figs. 1d and 2)?

Here, we combine in situ snow accumulation data and back trajectory modeling to examine the air-parcel trajectories associated with snowfall in the St. Elias (e.g., Eclipse Icefield) and Alaska (e.g., Begguya) Ranges, and their implications for historical accumulation records contained in the two ranges' glacier ice. Our work offers a new justification for interpreting multiple regional ice-core records in the context of one another, rather than as standalone climate histories.

2. Methods

2.1. Instrumental records of snow accumulation

Accumulation data were obtained from snow sounders at two different sites: the Kaskawulsh/Hubbard Divide (St. Elias Range) and Denali 14 Camp (Alaska Range). We use the term 'snow sounder' to refer to instruments used to measure changes in the snow surface position, from which accumulation and ablation can be calculated. To quantify snowfall conditions at each site, we define non-storm accumulation days (referred to as 'snow' days) to be days (defined midnight to midnight, local time) on which a surface change greater than 2 cm and less than 20 cm was detected, and 'storm' days when at least 20 cm of snow accumulated. We use a value of 20 cm within 24 hours as it is the threshold used by both Environment Canada and the United States National Weather Service for issuing public snowfall warnings (National Oceanic and Atmospheric Administration, 2009; Environment and Climate Change Canada, 2024). We use a threshold of 2 cm as our minimum detection limit for snowfall to account for instrumental error (noted below) and wind redistribution.

We calculate total snowfall by summing measured surface height increases, ignoring surface drops (e.g., due to surface melt, snow densification or wind redistribution). Although wind distribution may contribute to our measured surface height increases, its effect is likely small relative to snowfall, given the locations of our snow sounder sites away from any defined lee or stoss side of a ridge. Additionally, although we observe the effects of settling and compaction following snowfall events, we assume that these processes primarily affect snow surface height after a precipitation event is over, such that seasonal differences in these processes can be neglected when focusing, as we do, on surface changes during the event. We recognize, however, that the effects of both surface settling and wind redistribution remain uncontrolled sources of uncertainty in snowfall estimates for each snowfall event.

https://doi.org/10.1017/jog.2026.10142 Published online by Cambridge University Press

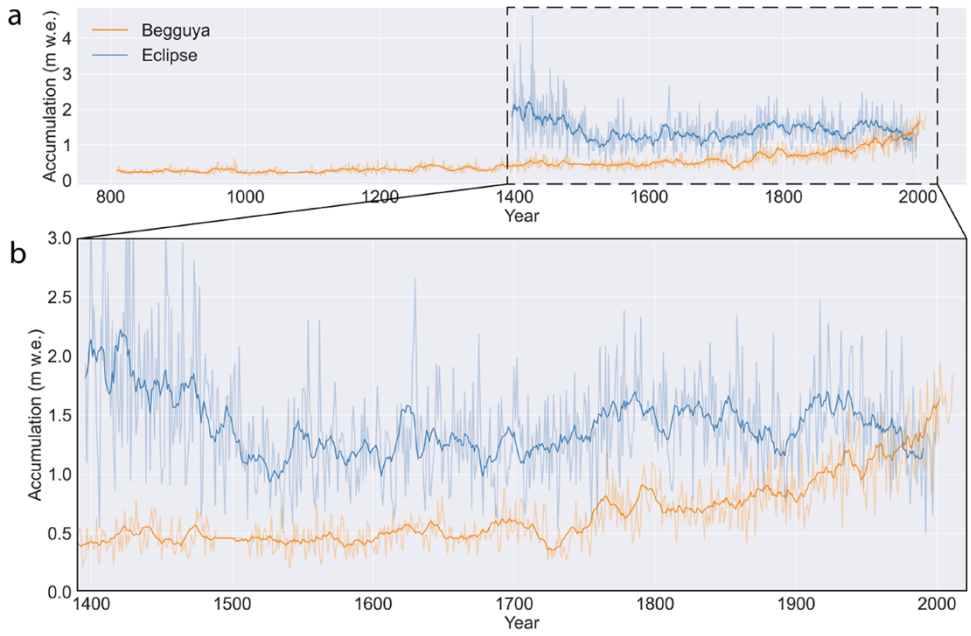

Figure 2. Ice-core accumulation records from Eclipse Icefield (blue; Kochtitzky and others, 2020) and Begguya (orange; Winski and others, 2017). Panel (b) shows a close-up of the dotted inset in panel (a) for the time period over which the two records overlap. Bolded lines show an 11-year smoothing.

To evaluate the representativeness of our temporally limited snow sounder data, we compare monthly accumulation from our snow sounder records to monthly ERA5 total precipitation over each site from 1940 to 2025. ERA5 has a footprint of 31 km, so it provides a spatially integrated estimate of precipitation in each of our two mountain ranges, rather than point measurements like our snow sounder data. We compare the two datasets, not to assess the accuracy of specific snow accumulation values, but to evaluate whether our snow sounder data are representative of the seasonal distribution of snowfall in each mountain range. Although ERA5 is not able to capture specific extreme precipitation events, it can generally capture spatial and temporal patterns of observed extratropical precipitation (Lavers and others, 2022).

2.1.1. The Kaskawulsh/Hubbard divide (St. Elias Range)

The Kaskawulsh/Hubbard Divide (60°42′N, 139°47′W; 2603 m a.s.l.) is situated in the accumulation zone near the top of Kaskawulsh and Hubbard Glaciers (Fig. 1). The Kaskawulsh/Hubbard snowfall record comprises twice-daily readings from a Campbell Scientific SR50 snow depth sounder covering the period from June 2003 to July 2012 obtained by . Instrumental accuracy is ±1 cm or 0.4% of the distance to the snow surface, whichever is greater (McConnell, 2019). Six (2004, 2005, 2006, 2008, 2009, 2011) of the 10 hydrological years in the record have at least partial (0–90%) coverage in all months (Fig. 3). We define hydrological years to run from 1 September to 31 August and designate them based on the calendar year in which they end (e.g., hydrological year 2003 runs from September 2002 through August 2003). We begin our hydrological years in September rather than October to better capture the autumn storm season (approximately September through December) that is characteristic of the region, as discussed below (Fig. 3).

2.1.2. Denali 14 camp (Alaska Range)

We obtained hourly accumulation data from a snow sounder at Denali's 14 200 ft climbers' camp ('14 Camp'; 63°04′N, 151°04′W; 4328 m a.s.l.; Fig. 1), which is located on the Kahiltna Glacier and sits ∼1700 m higher in elevation than the Kaskawulsh/Hubbard Divide. The 14 Camp snow accumulation record comprises hourly readings from a Campbell Scientific SR50a snow depth sounder covering the period from June 2018 to September 2023 (Fig. 3d). Instrumental accuracy is ±1 cm or 0.4% of the distance to the snow surface, whichever is greater. Of the seven hydrological years included in the 14 Camp record (2018–24), four of them (2019–22) have at least partial coverage during all months.

2.2. HYSPLIT atmospheric back trajectories

In order to determine whether and/or how air transport patterns differ between sites in the Alaska Range vs the St. Elias Range, we used NOAA's HYSPLIT trajectory model to run back trajectories for the atmospheric transport of moisture to three sites of interest in the St. Elias and Alaska Ranges (Fig. 1): the Kaskawulsh/Hubbard Divide, Eclipse Icefield ('Eclipse') and the Begguya summit plateau ('Begguya'). Eclipse and Begguya were chosen as they are sites in the region where ice cores have been recovered (Wake and others, 2002; Yalcin and others, 2007; Kelsey and others, 2012; Winski and others, 2017; 2018. Because the NCEP/NCAR meteorological data input to the HYSPLIT model has a resolution on a 2.5° × 2.5° lat/lon grid and 17 pressure levels from 1000 to 10 mb, we interpret trajectories for Begguya to be representative of trajectories to 14 Camp; the two sites are 15 km apart with 300 m difference in elevation (Fig. 1c). We also consider Eclipse and the Kaskawulsh/Hubbard Divide climatically analogous given our input data, as Eclipse is located 30 km from the Divide with a 400 m difference in elevation (Fig. 1d).

Interpretation of both Begguya and Eclipse ice-core records has to date relied on the assumption that snowfall at each of these sites is associated with transport of moisture from the Gulf of Alaska

https://doi.org/10.1017/jog.2026.10142 Published online by Cambridge University Press

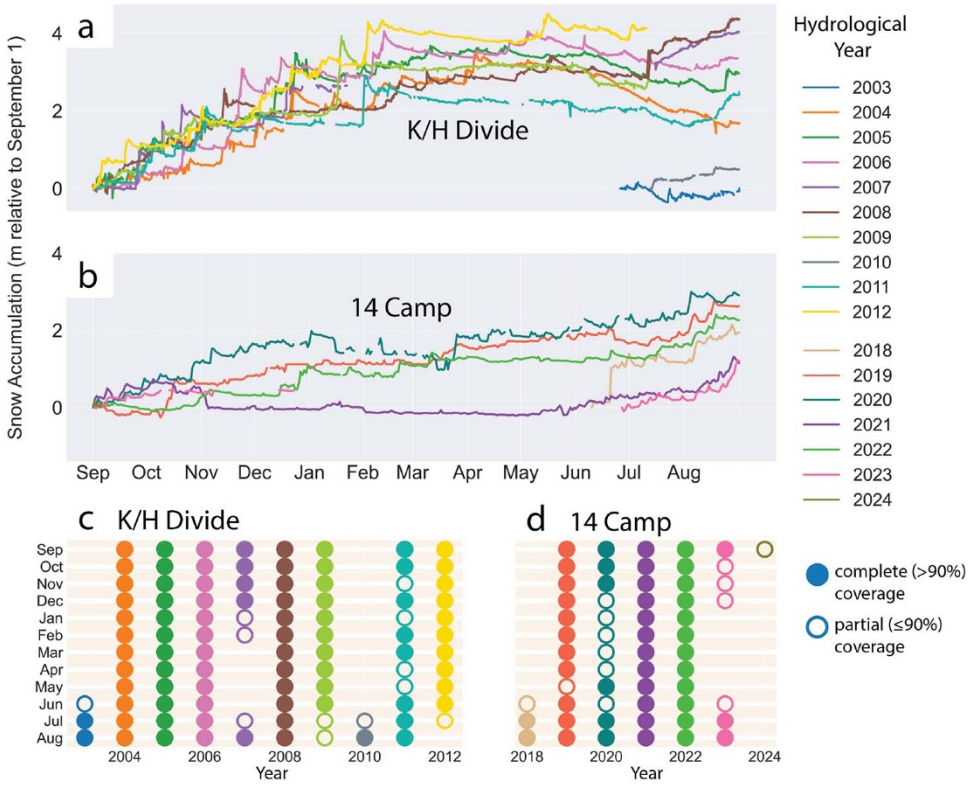

Figure 3. Instrumental records of snow accumulation from the Kaskawulsh/Hubbard Divide (a) and Denali 14 Camp (b). Accumulation is shown in meters relative to the first snow accumulation data point from each hydrological year represented. Panels (c) and (d) show the temporal coverage of the Divide and 14 Camp records, respectively.

to the ice-core site. However, accumulation and chemistry records differ between the two ice-core sites, implying that this simple model of inland moisture transport is not sufficient to describe snowfall and resultant chemical signals across the Gulf of Alaska region. Here, we use HYSPLIT to provide additional detail about air-parcel trajectories associated with snowfall in order to inform differences in the interpretation of ice-core records, focusing on accumulation records, from different sites in the Gulf of Alaska region.

Air-parcel back trajectories (four per day) were computed by the HYSPLIT atmospheric trajectory model between 1 January 1979 and 31 December 2019 using NCEP/NCAR v1 meteorological inputs. Each back trajectory position was computed at hourly time steps for a length of 10 days, beyond which we consider increasing model uncertainties to render outputs insufficiently meaningful.

Model outputs (latitude, longitude and air-parcel elevation values) were examined by month and by season for three snow conditions based on our snow sounder records: days without accumulation ('no-snow', $<$ 2 cm), days with non-storm accumulation ('snow', 2–20 cm) and storm days ('storm', $\geq$20 cm). In order to better isolate patterns associated with accumulation at the Kaskawulsh/Hubbard Divide, we identified no-snow, snow and storm days in the site's snow sounder record, both over the course of the entire year and also only within the months of September through December (SOND), when most accumulation occurs (Fig. 4). At 14 Camp, in contrast, we did not isolate September through December data, as snow accumulation is more evenly distributed throughout the year, as discussed below.

Finally, to contextualize our sites of interest in the broader Gulf of Alaska climate regime we identify years since 1979 with a particularly strong or weak Aleutian Low, and compare the HYSPLIT back trajectories for these years. The center position of the Aleutian Low is the average position of extratropical cyclones moving west to east across the North Pacific, and its location and intensity are primary indicators of wintertime North Pacific climate (Trenberth, 1990; Overland and others, 1999; Rodionov and others, 2007). We define years since 1979 with the bottom 20% of November–March North Pacific Index (the area-weighted sea level pressure over the region 30°N — 65°N, 160°E — 140°W;) values as strong Aleutian Low years, and years with the top 20% of North Pacific Index values as weak Aleutian Low years.

3. Results

We report results for each of our snow sounder sites individually, then discuss them in relation to one another. No-snow, snow and storm days at each snow sounder site are summarized in Table 1. When reporting and discussing results, we refer to the St. Elias Range (or 'St. Elias') and Alaska Range rather than individual snow sounder or ice-core sites since, as stated above, we view the snow sounder and ice-core sites in each range as climatically analogous. We use this language for clarity, recognizing that our results are not representative of each mountain range as a whole. Therefore, in the context of this paper, the term 'Alaska Range' should specifically be taken to mean 14 Camp and Begguya, and the term 'St. Elias Range' to mean the Kaskawulsh/Hubbard Divide and Eclipse.

https://doi.org/10.1017/jog.2026.10142 Published online by Cambridge University Press

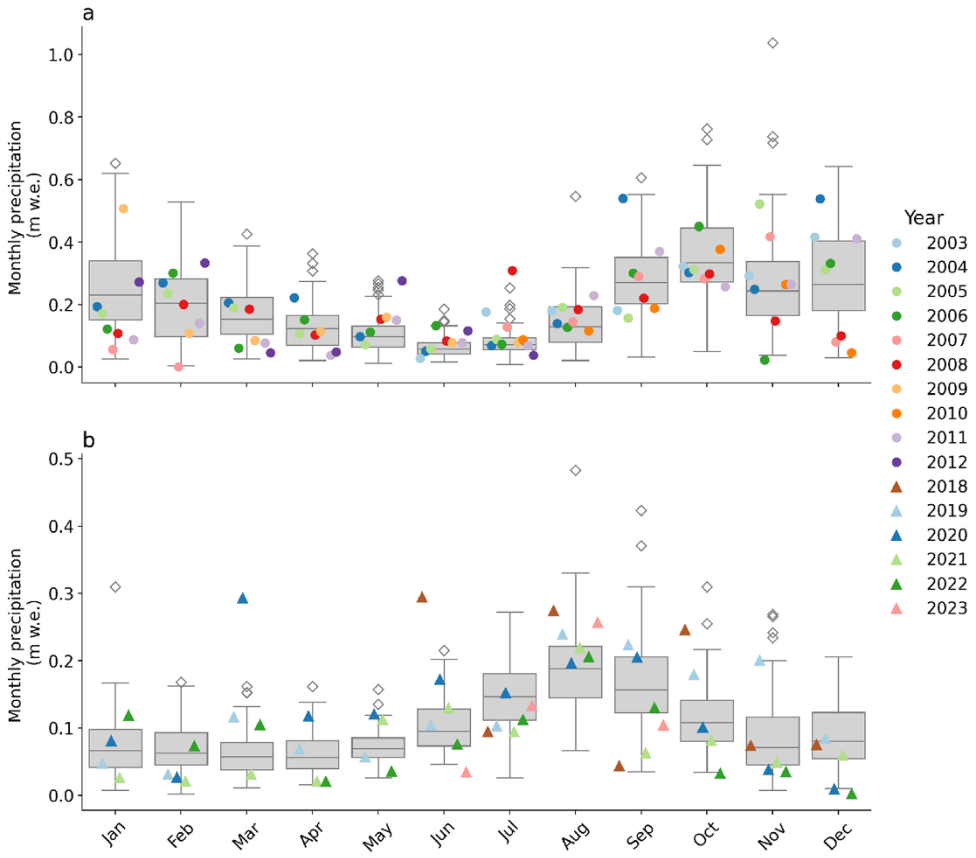

Figure 4. Monthly snow sounder accumulation from the St. Elias (Kaskawulsh/Hubbard Divide, (a)) and Alaska (14 Camp, (b)) Ranges compared with monthly ERA5 precipitation value from 1940 to 2025. Snow sounder data are shown with filled-in scatterpoints. ERA5 data are shown with boxplots with diamond-shaped outliers. We use a typical new-snow density value of 200 kg m^{-3} when converting snow sounder accumulation to m w.e. (Cuffey and Paterson, 2010).

3.1. Instrumental records of snow accumulation

Precipitation in the St. Elias is predominantly controlled by coastal storm systems moving inland from the Gulf of Alaska. Forty-four percent of annual accumulation in the St. Elias occurs in September through December, 40% of this during discrete storm events, despite storms occurring on only 2.6% of total September–December days on record (Fig. 3a).

Accumulation in the Alaska Range is more evenly distributed throughout the year than in the St. Elias; August receives, on average, the most snowfall, but there is no distinct fall/winter influx of accumulation (Figs. 3 and 4).

We do not have continuous in situ surface density measurements for converting monthly accumulation values from our snow sounders to meters w.e. for comparison with ERA5 precipitation (1940–2025). We therefore convert to m w.e. using three different values: 200 kg m^{-3} (typical new-snow density; Cuffey and Paterson, 2010), 470 kg m^{-3} (surface density measured at Eclipse; McConnell, 2019) and 400 kg m^{-3} (surface density measured at the Kaskawulsh/Hubbard Divide; Ochwat and others, 2021). When converted using 200 kg m^{-3}, monthly precipitation values from our snow sounder records generally fall within the range of ERA5 precipitation from 1940 to 2025. However, snow sounder monthly precipitation tends to be higher than ERA5 precipitation when converted using 470 and 400 kg m^{-3}. This may be a result of surface compaction between snowfall and measurement of surface density, an underestimation of precipitation in ERA5, or some combination. Regardless, seasonal patterns of snow accumulation are consistent between snow sounder data and ERA5 precipitation values at both sites (Fig. 4).

Table 1. No-snow, snow and storm days at snow sounder sites: Kaskawulsh/Hubbard (K/H) Divide and 14 Camp. No-snow days are defined as days with a surface increase of less than 2 cm. Snow days are defined as days with a surface increase between 2 and 20 cm. Storm days are defined as days with a surface increase of at least 20 cm in 24 hours.

	K/H Divide (annual)	K/H Divide (SOND)	14 Camp (annual)
Lat (°N)	60°42′	60°42′	63°04′
Lon (°W)	139°47′	139°47′	151°04′
Elevation (m a.s.l.)	2603	2603	4328
Snow days	969	396	338
% snow days	18.3%	21.0%	22.9%
Storm days	74	49	24
% storm days	1.4%	2.6%	1.6%
Total days with snowfall	1043	445	362
Total days in record	5281	1884	1475
% accumulation on storm days	31%	40%	22%
% accumulation on snow days	69%	60%	78%

3.2. HYSPLIT atmospheric back trajectories

HYSPLIT results demonstrate that the St. Elias tends to receive air parcels uplifted from lower elevations as they travel from the southwest, an effect that is amplified locally by the high relief coastline surrounding the Gulf of Alaska (Fig. 5). During the spring and summer, air parcels tend to arrive in the St. Elias from the Gulf

https://doi.org/10.1017/jog.2026.10142 Published online by Cambridge University Press

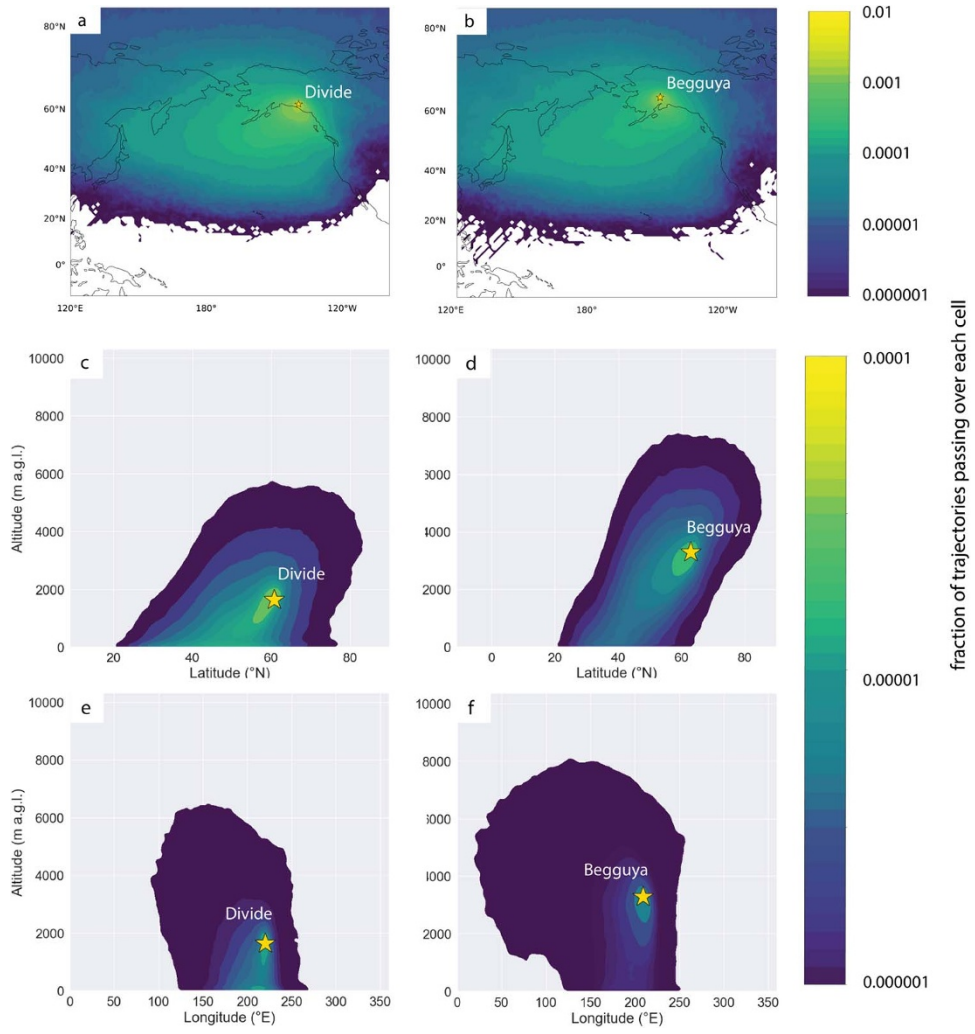

Figure 5. Fraction of HYSPLIT air trajectories passing through each $1^\circ \times 1^\circ$ (a–b) or $1^\circ \times 1$ m (c–f) parcel en route to the St. Elias Range and Alaska Ranges. Panels (a), (c) and (e) show latitude × longitude, latitude × altitude and longitude × altitude parcels for air parcels en route to the Kaskawulsh/Hubbard Divide. Panels (b), (d) and (f) show latitude × longitude, latitude × altitude and longitude × altitude parcels for air parcels en route to Begguya. The locations of the Kaskawulsh/Hubbard Divide and Begguya are marked by yellow stars in their respective panels. Note the log scale on the colorbar.

of Alaska and northern Pacific (Fig. S1a and b). In the fall, the area from which air parcels originate elongates across the Pacific toward Asia, then shifts south in the winter (Fig. S1c and d). We report the following patterns for no-snow vs snow vs storm days specifically for the months of September through December, when the St. Elias receives most of its snowfall. During no-snow days in the St. Elias, arriving air parcels do not follow any well-defined track (Fig. 6a). In contrast, during snow, and especially during storm, days in the St. Elias, arriving air parcels follow a distinct track inland from the Gulf of Alaska, with a more southerly source region during storm days, implicating the Gulf of Alaska and North Pacific as dominant moisture sources for St. Elias fall and winter storm events (Fig. 6c and e). Snow and storm days in most individual years conform to this pattern, with 2004 being the most notable exception (Figs S2 and S3). Individual storm tracks are shown in Fig. S4.

The Alaska Range also tends to receive air parcels uplifted from lower elevations as they travel from the southwest, indicating that most precipitation at the site is orographically induced (Fig. 5). Westerly trajectories toward the Alaska Range are more common in the summer than during other seasons (Fig. S1). The area from which air parcels arriving in the Alaska Range originate elongates across the Pacific toward Asia during the fall and winter relative to the summer (Fig. S1).

The strength of the Aleutian Low is an indicator of North Pacific wintertime climate, and HYSPLIT trajectories show that strong Aleutian Low conditions are associated with greater funneling of air parcels northwest from the Gulf of Alaska, while under a weaker Aleutian Low, the overall back-trajectory pattern is far more scattered, with comparatively more air parcels originating from a westerly direction in the Bering Sea region (Fig. 8).

4. Discussion

4.1. Regional snowfall comparisons: St. Elias vs Alaska Range

The results presented above highlight many similarities, but also some notable differences, between snowfall regimes and moisture sources in the Alaska and St. Elias Ranges. In both ranges, each large snowfall event is followed by a drop in snow surface height over the subsequent days, reflecting settling and compaction of the snowpack (Fig. 3a and b). Both the Alaska and St. Elias Ranges tend

https://doi.org/10.1017/jog.2026.10142 Published online by Cambridge University Press

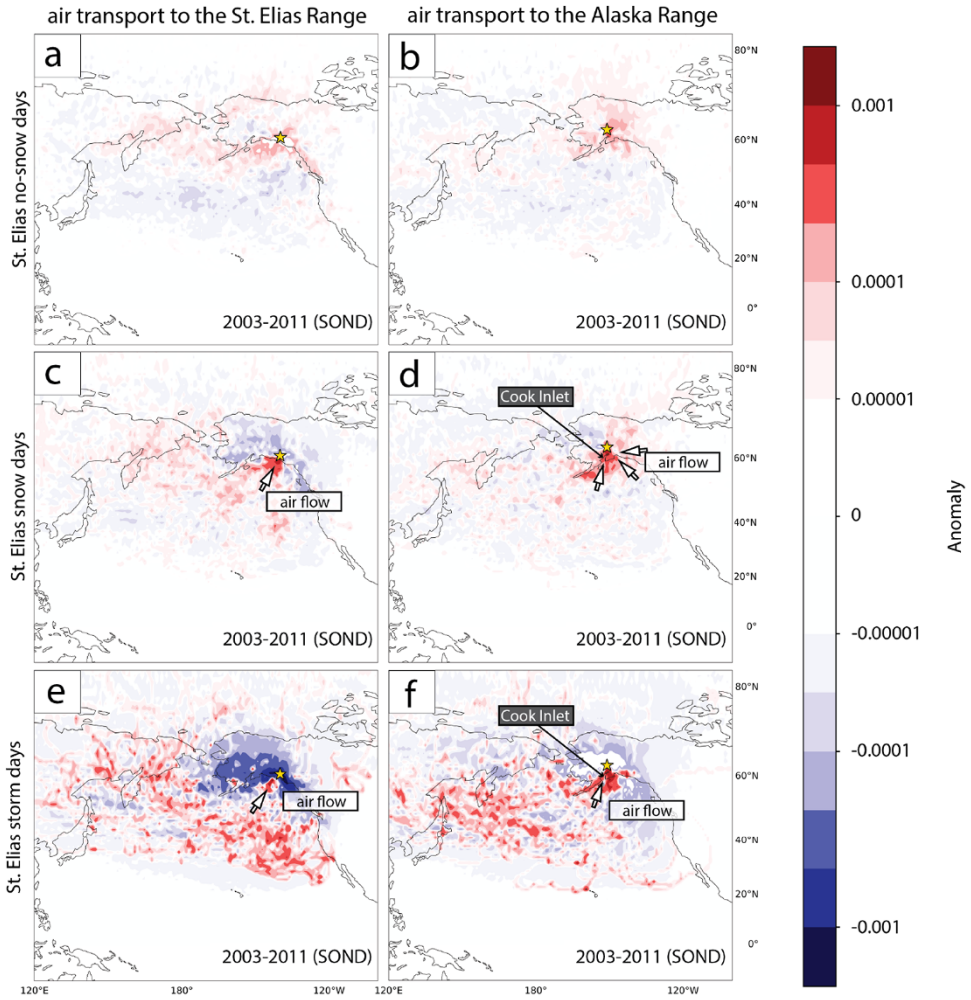

Figure 6. September through December air-parcel transport to the St. Elias and Alaska Ranges based on snowfall conditions at the Kaskawulsh/Hubbard Divide (St. Elias Range). For both the St. Elias and Alaska Ranges, HYSPLIT air-parcel trajectory anomalies over each $1^\circ \times 1^\circ$ parcel are shown leading to no-snow (a–b), snow (c–d) and storm (e–f) days recorded at the Kaskawulsh/Hubbard Divide (marked by a yellow star). The anomaly for each parcel is calculated relative to the fraction of air mass trajectories passing over that parcel under all snow conditions. The dominant patterns of airflow (as visually identified) that precede each snowfall condition at the Kaskawulsh/Hubbard Divide are shown by white arrows. Note the log scale on the colorbar.

to receive air parcels uplifted from lower elevations as they travel from the southwest, indicating orographic precipitation. For both ranges, the area from which arriving air parcels originate elongates across the Pacific toward Asia during the fall and winter relative to the summer.

Accumulation zone snowfall records from the St. Elias and Alaska Ranges show a clear distinction between maritime and continental climate regimes, respectively. The St. Elias Range's proximity to the Gulf of Alaska makes it more sensitive to the fall and winter weather systems that develop offshore and move inland; we find that 44% of annual snow accumulation in the St. Elias falls in the months of September through December, often accumulating in discrete storm events. In contrast, the Alaska Range is located in the Alaskan interior and shows an annual snowfall distribution less dominated by fall and winter storms originating from the Gulf of Alaska, with only 35% of annual accumulation occurring during September–December.

Overall mean annual accumulation (given in meters water equivalent calculated with a snow density value of 200 kg m^{-3}; Cuffey and Paterson, 2010) is not significantly different between the St. Elias (0.59 ± 0.17 m w.e.) and Alaska Ranges (0.45 ± 0.13 m w.e.), though without temporal overlap in the snow sounder records from the two sites no direct comparison can be made. Modeled regional precipitation in Alaska and the Yukon (Newman and others, 2020) shows near-maximum levels in both the St. Elias and Alaska Ranges, although the zone of maximum precipitation is much more restricted in the Alaska Range compared to the St. Elias.

Combined HYSPLIT results from the St. Elias and Alaska Ranges suggest that while both locations are impacted similarly by large storm systems moving inland from the Gulf of Alaska, non-storm accumulation in the two ranges differs and is largely governed by orography (Figs. 1b, 6 and 7). During snow days in the St. Elias, trajectories for the range come predominantly from the south, moving inland from the Gulf of Alaska, similar to during storm days but less defined (Fig. 6c). Concurrent trajectories for the Alaska Range, in contrast, are more dispersed (Fig. 6d), suggesting that while weather systems moving in from the Gulf of Alaska dominate both storm and non-storm accumulation in the St. Elias, many smaller coastal systems weaken before reaching the interior.

At Cook Inlet, however, there is an approximately 100 km gap in the modeled coastal high-precipitation band, north of which sits

https://doi.org/10.1017/jog.2026.10142 Published online by Cambridge University Press

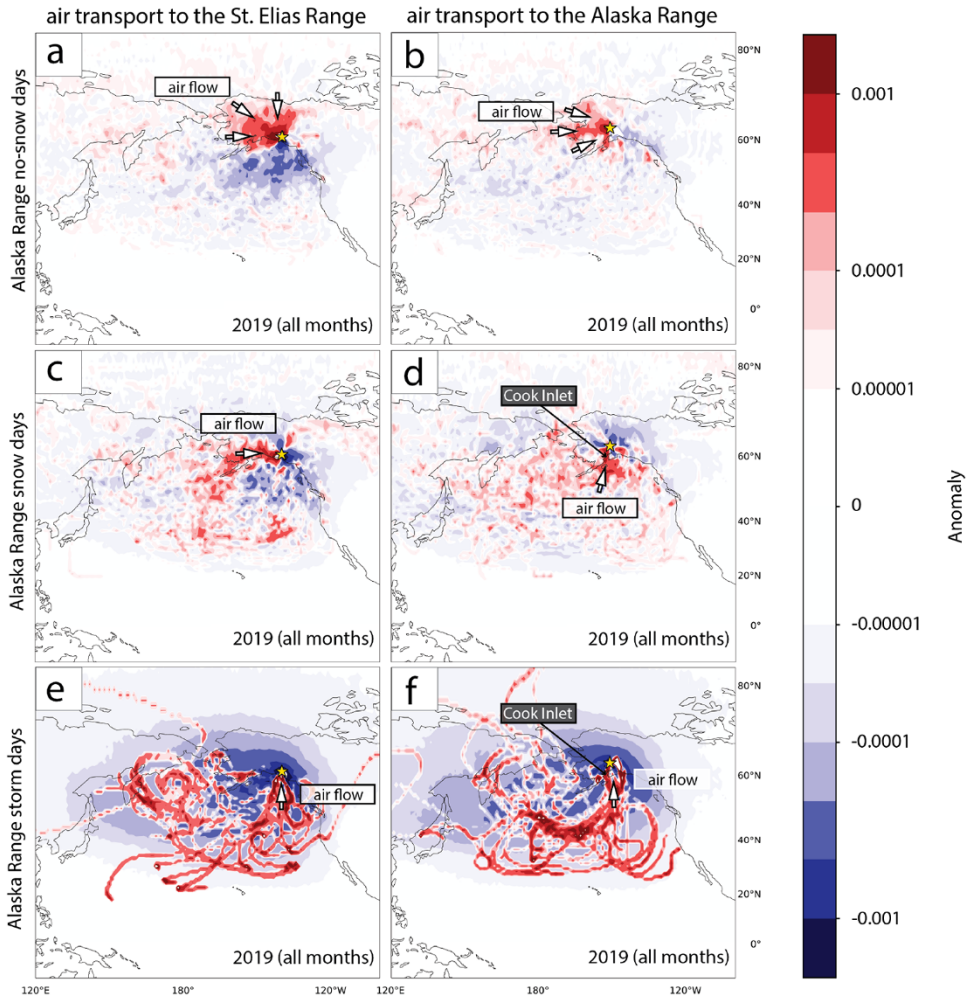

Figure 7. Air-parcel transport to the St. Elias and Alaska Ranges based on snowfall conditions at 14 Camp (Alaska Range). For both the St. Elias and Alaska Ranges, HYSPLIT air-parcel trajectory anomalies over each $1^\circ \times 1^\circ$ parcel are shown leading to no-snow (a–b), snow (c–d) and storm (e–f) days recorded at 14 Camp (marked by a yellow star). The anomaly for each parcel is calculated relative to the fraction of air mass trajectories passing over that parcel under all snow conditions. The dominant patterns of airflow (as visually identified) that precede each snowfall condition at 14 Camp are shown by white arrows. Note the log scale on the colorbar.

the Alaska Range, where another, smaller zone of high precipitation is located (Newman and others, 2020). Our results support the idea that when non-storm coastal systems do reach the Alaska Range, they do so where Cook Inlet cuts through the coastal mountains (Fig. 7). Because there is no comparable feature cutting through the coastal peaks between the Gulf of Alaska and the interior St. Elias icefields, small weather systems may be blocked from reaching the Kaskawulsh/Hubbard Divide even if they are able to access the Alaska Range. The lack of southerly air-parcel trajectories in the St. Elias associated with non-storm snowfall in the Alaska Range is consistent with this idea.

4.2. *The Aleutian Low and Gulf of Alaska precipitation regime*

HYSPLIT trajectories for storm days recorded at our two snow sounder sites show similar trajectories in both the St. Elias and Alaska Ranges (Figs. 6e and f and 7e and f). The importance of large Gulf of Alaska storm systems to regional climate can also be seen in the HYSPLIT trajectories during periods of a strong vs weak Aleutian Low (Fig. 8). Each year, the Aleutian Low undergoes a seasonal westward migration; in early fall, storm deepening occurs primarily in the Gulf of Alaska, while in late fall it shifts south of Kamchatka (Pickart and others, 2009). This migration is reflected in the seasonal westward shift in HYSPLIT trajectories to both the St. Elias and Alaska Ranges (Fig. S1).

A stronger Aleutian Low can occur as a result of increased duration or strength of individual storms, increased storm frequency, greater coherence between individual storm trajectories to a well-defined track, or some combination of the three, complicating the relationship between the Aleutian Low and regional snow accumulation. Generally, strong Aleutian Low conditions are associated with more storms of high intensity and a well-defined storm track compared to weak Aleutian Low conditions (Rodionov and others, 2007; Zhu and others, 2007). HYSPLIT trajectories to both the St. Elias and Alaska Ranges are indeed much more coherent under a strong Aleutian Low, when air parcels are funneled in from the south and southeast, off the Gulf of Alaska (Fig. 8). Conversely, under a weak Aleutian Low, air-parcel trajectories are more dispersed. Our results suggest that a 'typical' strong Aleutian Low, characterized by more storms of high intensity, leads to snowfall in the Gulf of Alaska region, more defined by the size and frequency of storm events and less moderated by regional topography. Under this type of strong Aleutian Low, the position

https://doi.org/10.1017/jog.2026.10142 Published online by Cambridge University Press

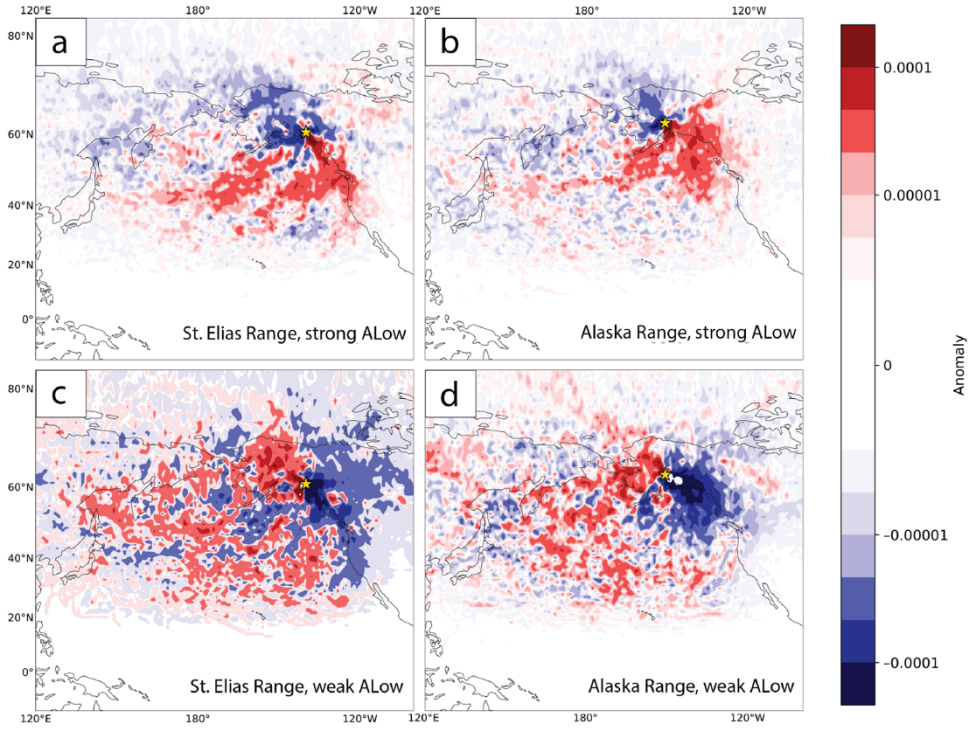

Figure 8. Air-parcel trajectories during years with a strong and weak Aleutian Low defined by anomalies from the 1925–89 mean (Trenberth and Hurrell, 1994b). Anomaly plots of the fraction of trajectories passing over each $1^\circ \times 1^\circ$ parcel are shown for the St. Elias Range (Kaskawulsh/Hubbard Divide; a, c) and to the Alaska Range (Begguya; b, d). The anomaly for each parcel is calculated relative to the fraction of air mass trajectories passing over that parcel under all snow conditions. Each back-trajectory starting cell is marked by a yellow star. Note the log scale on the colorbar, which is different than the log scale on all the snow condition anomaly plots.

of the dominant storm track may be less important, as large storm systems affect both coastal and interior sectors. Conversely, a 'typical' weak Aleutian Low, characterized by a higher proportion of non-storm accumulation, leads to greater topographic moderation of snowfall in the Gulf of Alaska region. Under this type of weak Aleutian Low, storm track position and interaction with topography play a comparatively more important role in controlling the regional distribution of snow accumulation.

The future of the Gulf of Alaska precipitation regime will be largely determined by the future of stormy weather in the region. A northward shift and intensification of the Aleutian Low, and specifically an intensification of extreme Aleutian Low events, is projected under IPCC scenario RCP8.5 (Gan and others, 2017; Giamalaki and others, 2021). A northward shift of the Aleutian Low center aligns slightly more closely with storm trajectories toward the St. Elias than the Alaska Range (Figs. 6 and 7). A more intense Aleutian Low likely means more storms of higher intensity funneled inland from the Gulf of Alaska, which would increase snowfall throughout the region, even on areas sheltered by orographic barriers during less intense snow events.

4.3. Implications for ice-core records

The difference we see in St. Elias and Alaska Range accumulation patterns suggests that interpreting ice-core accumulation records from the two locations in the context of one another can prove a powerful tool for untangling past patterns of air-parcel movement. Our HYSPLIT results show the most distinct air-parcel trajectories on storm days, which are associated with southerly storm tracks moving inland from the Gulf of Alaska toward both the St. Elias and Alaska Ranges. Although neither of the sites show a single defined air-parcel trajectory for non-storm snow days, they do demonstrate patterns of air transport distinct from each other: snow days in the St. Elias are associated with southerly trajectories in both the St. Elias and Alaska Ranges, indicating southerly transport of storm systems strong enough to carry moisture over the first band of coastal high peaks, reaching the rest of the St. Elias and the Alaska Range. In contrast, snow days in the Alaska Range are associated with southerly trajectories in the Alaska Range but not the St. Elias, indicating blockage of air parcels by the first band of high coastal peaks except where Cook Inlet cuts through.

Using two or more accumulation records in combination therefore provides insight into air parcel trajectories beyond the major storm events that dominate the accumulation signal during stormy years. For example, combining our HYSPLIT results with the ice-core accumulation records from both Begguya (Alaska Range) and Eclipse (St. Elias Range) can narrow the list of likely mechanisms for the increase in Begguya accumulation reported by . Non-storm snowfall in the St. Elias is more reliant on system strength, whereas non-storm snowfall in the Alaska Range is more reliant on system trajectory, in particular on where storm systems encounter the coastal mountains. Eclipse is thus likely affected by a higher proportion of midsize systems not strong enough to impact the entire region (i.e., not strong enough to make it to the Alaska Range), but strong enough to cross the high coastal peaks without dropping all their moisture. In contrast, small and midsize systems can both reach Begguya so long as their trajectories cut through the coastal mountains at Cook Inlet. Our HYSPLIT results suggest the increase in Begguya accumulation, and concurrent decrease in Eclipse accumulation, from 1400 to 2000 C.E. may be explained by a shift in dominant air-parcel trajectory, or a coalescing of

https://doi.org/10.1017/jog.2026.10142 Published online by Cambridge University Press

air-parcel trajectories to a well-defined track that cuts through Cook Inlet, rather than an increase in average storm strength or frequency.

4.4. Data limitations and value

The biggest limitation of our results arises from the restricted temporal coverage and lack of overlap between our two snow sounder datasets. This precludes direct comparison of snowfall values themselves, as well as of atmospheric conditions associated with snowfall in any given year. However, we consider each record individually a unique and valuable characterization of local snow accumulation, as only in situ measurements such as these can provide daily, event-resolved accumulation data. The Kaskawulsh/Hubbard Divide record, in particular, provides an unparalleled quantification, with seven years of near-complete coverage of the local snowfall regime dominated by fall and winter accumulation, a phenomenon that is well known anecdotally, but to date has received limited documentation. Similarly, 14 Camp has been well observed anecdotally by climbers to receive significant summertime accumulation, but this, to date, has remained largely unquantified. In fact, local event-resolved accumulation data are largely unavailable in alpine regions worldwide because of the challenges associated with deploying and maintaining instrumentation. Our results, therefore, not only provide a valuable quantitative basis for previous anecdotal understanding of local conditions in alpine terrain, but are unique in doing so.

Furthermore, monthly accumulation values from our snow sounder records are generally consistent with ERA5 precipitation from 1940 to 2025, and seasonal patterns of snow accumulation are consistent between snow sounder data and ERA5 precipitation values at both sites (Fig. 4).

Finally, the majority of individual years covered by the Kaskawulsh/Hubbard Divide accumulation record show consistent atmospheric back trajectories associated with snow and storm days. Based on the consistent trajectories associated with snow days at the Kaskawulsh/Hubbard Divide combined with the reasonable seasonal distribution and monthly accumulation totals at both sites, we consider the patterns observed over our in situ records representative of general snowfall conditions at each site.

5. Conclusions

Orographic effects are a defining feature of atmospheric transport in the Gulf of Alaska region and account for a clear distinction between maritime and continental climate regimes. For example, snow accumulation in the St. Elias Range is dominated by September–December storm events, while accumulation in the Alaska Range is more evenly distributed throughout the year. Although orographic effects are ever present, their influence is greatest during non-storm accumulation events, during which southerly air parcels tend to either bring moisture to the Kaskawulsh/Hubbard Divide (St. Elias Range) but dry out before reaching 14 Camp (Alaska Range), or bring moisture to 14 Camp via Cook Inlet but be blocked from reaching the Kaskawulsh/Hubbard Divide by the nearby high coastal St. Elias peaks. In contrast, storm-day accumulation at sites in both the St. Elias and Alaska Ranges is associated with southerly airflow inland from the Gulf of Alaska.

Results suggest that the future of the Gulf of Alaska precipitation regime will be largely determined by the evolution of stormy weather in the region. Projected intensification of the Aleutian Low (Giamalaki and others, 2021) likely means more storms of higher intensity funneled inland from the Gulf of Alaska, generally increasing precipitation in the region. However, local high-alpine increases in snow accumulation associated with more storms of higher intensity may either be amplified or offset by changes in non-storm accumulation associated with changes in the dominant pathways of air-parcel transport.

Finally, results support the interpretation of ice cores from the St. Elias Range in terms of regional (maritime) climate, and provide insight into differences between St. Elias and Alaska Range ice-core accumulation records. In particular, our HYSPLIT results suggest that the divergent behavior between Begguya and Eclipse ice-core accumulation records from ∼1400 to 2000 C.E. may be explained by a shift in dominant air-parcel trajectory, or a coalescing of air-parcel trajectories to a well-defined track that cuts through Cook Inlet, rather than an increase in average storm strength or frequency.

Our study highlights the value of in situ accumulation records from alpine regions and their contribution of daily, event-resolved snowfall data from regions where such observations are exceedingly rare.

Supplementary material. The supplementary material for this article can be found at https://doi.org/10.1017/jog.2026.10142.

Acknowledgements. We dedicate this paper to Bea Alt (formerlyTaylor-Barge), a pioneering researcher in alpine and polar climatology, who first carried out field investigations in the St. Elias Mountains in the mid-1960s during the Icefield Ranges Research Program. We thank the Tanana people, as well as the Kluane, Champagne and Aishihik, and White River First Nations, on whose traditional territories our snow sounders were deployed. We thank Denali National Park, Kluane National Park and Reserve (ParksCanada), Icefield Discovery, Kluane Lake Research Station, Talkeetna Air Taxi, Jean Bjornson and NSF logistics providers for collaboration and support. We thank the Denali National Park and Preserve South District Mountaineering Rangers, with whom ML has partnered for many years to collect the Kahiltna Glacier weather data.

Funding statement. Funding for this work was provided by the U.S. National Science Foundation, including awards 2002470,OPP-0136005, 0240878, 0713974, and AGS1203838, 1502783, 1806422, and 2002483. We are also grateful for funding from the Natural Sciences and Engineering Research Council of Canada, ArcticNet Network of Centres of Excellence Canada, Geological Survey of Canada, Polar Continental Shelf Program and University of Ottawa. Snow sounders at 14Camp and Base Camp were supported in large part by the Glacier Monitoring Program of the NPS Inventory and Monitoring Program.

References

Bieniek PA and 14 others (2012) Climate divisions for alaska based on objective methods. *Journal of Applied Meteorology and Climatology* **51**(7), 1276–1289. doi:10.1175/JAMC-D-11-0168.1.

Cuffey KM and Paterson WSB (2010) *The Physics of Glaciers*, 4th Edn. Elsevier.

Environment and Climate Change Canada (2024) Criteria for Public Weather Alerts.

Fang L and 9 others (2023) Early Holocene ice on the Begguya plateau (Mt. Hunter, Alaska) revealed by ice core 14c age constraints. *Cryosphere* **17**, 4007–4020. doi:10.5194/TC-17-4007-2023.

Farinotti D and 6 others (2019) A consensus estimate for the ice thickness distribution of all glaciers on Earth. *Nature Geoscience* **12**, 168–173. doi:10.1038/S41561-019-0300-3.

Fisher DA and 20 others (2004) Stable isotope records from Mount Logan, Eclipse ice cores and nearby Jellybean Lake. Water cycle of the North Pacific

over 2000 years and over five vertical kilometres: Sudden shifts and tropical connections. *Geographie Physique et Quaternaire* **58**(2), 337–352. doi:10.7202/013147AR.

Gan B and 7 others (2017) On the response of the aleutian low to greenhouse warming. *Journal of Climate* **30**(10), 3907–3925. doi:10.1175/JCLI-D-15-0789.1.

Giamalaki K, Beaulieu C, Henson SA, Martin AP, Kassem H and Faranda D (2021) Future intensification of extreme Aleutian Low events and their climate impacts. *Scientific Reports* **11**(1), 1–12. doi:10.1038/S41598-021-97615-7.

Kelsey EP, Wake CP, Yalcin K and Kreutz K (2012) Eclipse ice core accumulation and stable isotope variability as an indicator of North Pacific climate. *Journal of Climate* **25**(18), 6426–6440. doi:10.1175/JCLI-D-11-00389.1.

Kochtitzky W and 9 others (2020) Climate and surging of Donjek glacier, Yukon, Canada. *Arctic, Antarctic, and Alpine Research* **52**(1), 264–280. doi:10.1080/15230430.2020.1744397.

Lavers DA, Simmons A, Vamborg F and Rodwell MJ (2022) An evaluation of era5 precipitation for climate monitoring. *Quarterly Journal of the Royal Meteorological Society* **148**(748), 3152–3165. doi:10.1002/QJ.4351;CTYPE:STRING:JOURNAL.

Marcus MG and Ragle RH (1970) Arctic and alpine research snow accumulation in the Icefield Ranges, St. Elias Mountains, Yukon. **2**(4), 277–292. doi:10.1080/00040851.1970.12003587.

McConnell EA (2019) *Mechanisms of Ice Core Stable Isotope Variability in the Upper Kaskawulsh-Donjek Region, St. Elias Mountains, Yukon, Canada.* Master's thesis, University of Maine.

National Oceanic and Atmospheric Administration (2009) National Weather Service Glossary.

Newman AJ, Clark MP, Wood AW and Arnold JR (2020) Probabilistic spatial meteorological estimates for Alaska and the Yukon. *Journal of Geophysical Research: Atmospheres* **125**(22), e2020JD032696. doi:10.1029/2020JD032696.

Ochwat NE, Marshall SJ, Moorman BJ, Criscitiello AS and Copland L (2021) Evolution of the firn pack of Kaskawulsh Glacier, Yukon: Meltwater effects, densification, and the development of a perennial firn aquifer. *Cryosphere* **15**(4). doi:10.5194/TC-15-2021-2021.

Osterberg EC and 8 others (2017) The 1200-year composite ice core record of Aleutian Low intensification. *Geophysical Research Letters* **44**(14), 7447–7454. doi:10.1002/2017GL073697.

Overland JE, Adams JM and Bond NA (1999) Decadal variability of the Aleutian Low and its relation to high-latitude circulation. *Journal of Climate* **12**(5), 1542–1548. doi:10.1175/1520-0442(1999)012<1542:DVOTAL>2.0.CO;2.

Pickart RS, Moore GW, Macdonald AM, Renfrew IA, Walsh JE and Kessler WS (2009) Seasonal evolution of Aleutian low pressure systems: Implications for the North Pacific subpolar circulation. *Journal of Physical Oceanography* **39**(6), 1317–1339. doi:10.1175/2008JPO3891.1.

Rodionov SN, Bond NA and Overland JE (2007) The Aleutian Low, storm tracks, and winter climate variability in the Bering Sea. *Deep-Sea Research II* **54**(23-26), 2560–2577. doi:10.1016/j.dsr2.2007.08.002.

Trenberth K (1990) Recent observed Interdecadal climate changes in the Northern Hemisphere. *Bulletin of the American Meteorlogical Society* **71**(7), 988–993.

Trenberth KE and Hurrell JW (1994a) Decadal atmosphere-ocean variations in the pacific. *Climate Dynamics* **9**(6), 303–319. doi:10.1007/BF00204745.

Trenberth KE and Hurrell JW (1994b) Np Index data. Provided by the Climate Analysis Section. NCAR. (accessed 02 November 2023).

Tsushima A and 6 others (2015) Reconstruction of recent climate change in Alaska from the Aurora Peak ice core, central Alaska. *Climate of the Past* **11**, 217–226. doi:10.5194/cp-11-217-2015.

Wake CP, Yalcin K and Gundestrup NS (2002) The climate signal recorded in the oxygen-isotope, accumulation and major-ion time series from the Eclipse ice core, Yukon Territory, Canada. *Annals of Glaciology* **35**, 416–422. doi:10.3189/172756402781817266.

Winski D and 10 others (2017) Industrial-age doubling of snow accumulation in the Alaska Range linked to tropical ocean warming. *Scientific Reports* **7**(1), 17869. doi:10.1038/s41598-017-18022-5.

Winski D and 10 others (2018) A 400-year ice core melt layer record of summertime warming in the Alaska Range. *Journal of Geophysical Research: Atmospheres* **123**(7), 3594–3611. doi:10.1002/2017JD027539.

Yalcin K, Wake CP, Kreutz KJ, Germani MS and Whitlow SL (2007) Ice core paleovolcanic records from the St. Elias Mountains, Yukon, Canada. *Journal of Geophysical Research: Atmospheres* **112**(D8), D08102. doi:10.1029/2006JD007497.

Zdanowicz C and 12 others (2014) Ice cores from the St. Elias mountains, Yukon, Canada: Their significance for climate, atmospheric composition and volcanism in the North Pacific region. *Arctic* **67**, 35–57. doi:10.14430/arctic4352.

Zhu X, Sun J, Liu Z, Liu Q and Martin JE (2007) A synoptic analysis of the interannual variability of winter cyclone activity in the Aleutian Low region. *Journal of Climate* **20**(8), 1523–1538. doi:10.1175/JCLI4077.1.

https://doi.org/10.1017/jog.2026.10142 Published online by Cambridge University Press